PHYSICAL REVIEW B **88**, 125144 (2013)

Coherence of a sliding charge-density wave stimulated by asynchronous rf irradiation

S. G. Zybtsev and V. Ya. Pokrovskii*

Kotel'nikov Institute of Radioengineering and Electronics of the Russian Academy of Sciences, Mokhovaya 11-7, 125009 Moscow, Russia

(Received 15 July 2013; revised manuscript received 5 September 2013; published 30 September 2013)

We show that rf irradiation drastically increases coherence of the charge-density wave (CDW) depinning and sliding in the electric field for NbS_3 (phase II), TaS_3, and $(TaSe_4)_2I$. The effect is observed in the range of the CDW currents at which the fundamental frequencies are well below the frequency of the irradiation. The result is evident from the shape of I-V curves, Shapiro steps, and noise spectra. We treat the effect in terms of the rf-assisted relaxation of metastable states forming at CDW sliding. The rf irradiation can be helpful in experiments, where utmost coherence of the CDW transport is needed, e.g., in studies of the Shapiro steps, expanding the ranges of their observation.

DOI: 10.1103/PhysRevB.88.125144 PACS number(s): 71.45.Lr, 78.70.Gq

I. INTRODUCTION

Sliding of the charge-density wave (CDW), i.e., the Fröhlich mode of electronic transport, is the central and most discriminating feature of quasi-one-dimensional conductors below the Peierls transition temperature.[1] The sliding is observed at electric fields exceeding the threshold value E_t and is accompanied by low-frequency broadband electric noise (BBN) and narrowband noise (NBN) typically in rf or hf ranges. The NBN reflects sliding of the CDW in a periodic pinning potential or phase slippage at the contacts.[2,3] In the majority of the models, the NBN frequency f_f equals the inverse time of the CDW advancement by one wavelength λ and is usually referred to as "fundamental" or "washboard".

The collective electronic transport and the NBN generation can be characterized in terms of the CDW coherence and homogeneity of the CDW in space and in time. The coherence can be affected by external rf (or hf) irradiation. The most widely studied effect of the irradiation is the synchronization of the CDW, known also as the interference effect, mode locking, or the Shapiro steps. Suppose, at a certain voltage, V above the threshold value V_t, the frequency f_f or one of its harmonics or subharmonics, coincides with the frequency of the RF irradiation. Then the current-voltage dependence, $I(V)$, exhibits an interval where the current of the CDW is constant, i.e., the so-called Shapiro step. Correspondingly, a peak of $R_d \equiv dV/dI$ (or a dip of $\sigma_d \equiv dI/dV$) appears on its dependence on V. Below, we also call it a Shapiro step or a Shapiro peak. To explain the effect simply, the external rf field dictates sliding of the CDW with a given velocity in a certain voltage range, and the differential resistance of the CDW increases (up to infinity with complete synchronization).

While the synchronization effects have been widely studied,[4] almost no attention has been paid to the effects of rf irradiation when its frequency f is different from or, particularly, much higher than f_f and its harmonics in the voltage range studied. Meanwhile, one can notice that rf irradiation affects the shape of the I-V curves not only in the regions of Shapiro steps. As an example, one can mention the obvious reduction of E_t with the rf amplitude increase observed in all the interference experiments (see Fig. 4.2 from Ref. 4, for example). However, no studies of the effects of rf radiation beyond the regions of synchronization have been performed up to now.

In this paper we present studies of the effects of rf irradiations at relatively high frequencies, $f \gg f_f$. We show, that the irradiation not only decreases the value of E_t but also strongly changes the shape of $\sigma_d(E)$ curves above E_t: the growth of σ_d with E becomes sharper, the Shapiro steps (induced by another rf source) become more pronounced, the level of BBN drops, and the NBN lines in the noise spectra become narrower. This means that the CDW depinning becomes more "unanimous," and transport becomes much more coherent. The coherence of the CDW increases with the growth of f up to ~5 GHz at least. We associate the effect with the rf-stimulated relaxation of the internal strains of the sliding CDW.

We have studied $R_d(V)$ curves of three different CDW compounds: NbS_3 (phase II), TaS_3, and $(TaSe_4)_2I$ under "*cohering*" rf irradiation. The most detailed results were obtained for NbS_3, which needs special introduction. The second phase of this compound shows three CDW transitions: at $T_{P1} = 330$–370 K, $T_{P2} = 150$ K, and T_{P0} above 600 K.[1,5,6] Sliding of the CDWs forming below T_{P1} and T_{P2} has been reported. In particular, at room temperature NbS_3 shows highly coherent CDW transport indicated by the Shapiro steps; the highest frequency of synchronization is 17 GHz.[7] Here, we present the studies of the room-temperature CDW in NbS_3.

The arrangement of the paper is as follows. First, we introduce some details of the experimental techniques, including simultaneous application of two rf sources to a sample (Sec. II). Then, we separately consider the effect of low-frequency ac voltage (below 50 MHz) on the I-V curves (Sec. III). At these frequencies, the voltage across the sample can be directly measured. This study allows observation of the crossover from trivial smearing out of the I-V curves to the effect of coherence stimulation. Section IV concerns the effect of rf irradiation up to the gigahertz range on the shape of the I-V curves of NbS_3. In Sec. V, we report the stimulation of CDW coherence in NbS_3 probed with the help of another rf source. Section VI demonstrates the universality of the effect: the data for $(TaSe_4)_2I$ and TaS_3 are presented. In Sec. VII, we report the effects of the irradiation on the NBN and BBN generation. Section VIII is devoted to the discussion of the physics of the effect and its applications for the CDW studies.

II. EXPERIMENTAL DETAILS

Shapiro steps can give clear evidence of the coherence or incoherence of the CDW sliding. Therefore, in some of the experiments, we applied two rf generators to the samples simultaneously in parallel: the first one to stimulate the coherence and the second to probe this coherence through the Shapiro steps. Below, we refer to the second source as "*synchronizing*" voltage to distinguish it from the first one, cohering rf irradiation, applied at higher frequencies.

Small samples (<0.1 μm^2 in cross section) were selected for the experiment, because the CDW shows higher coherence therein.[8,9]

The best way to compare the effects of rf at different frequencies is to apply the cohering rf voltages of equal amplitudes. However, the absolute value of the ac voltage across the sample could be measured only at relatively low frequencies, up to ~50 MHz. At the highest frequencies, the rf voltage could not be measured directly because of the uncontrollable losses in the cables and poor matching with samples. However, we avoided this problem involving the effect of threshold suppression under rf irradiation. Typically, with the growth of rf power, E_t decreases, while the value of low-field conductivity remains approximately the same. Further growth of power results in reduction of E_t down to zero, and then the zero-field conductivity begins to grow. This very effect was used for tuning the rf power at different frequencies. To compare the shapes of $\sigma_d(V)$ curves at different rf frequencies, we usually set the power suppressing E_t down to zero, keeping $\sigma_d(0)$ unchanged. In some other cases, we confronted the effects of different frequencies at the same degree of E_t suppression. As we will see below, the shape of the $\sigma_d(V)$ curves above V_t is dominated by the irradiation frequency, rather than amplitude: if one plots $\sigma_d(V\text{-}V_t)$ for a completely or half-suppressed threshold, the curves will be approximately the same. Of course, with such criteria, we can make only qualitative conclusions about the effects of rf.

The invariability of low-field conductivity at different conditions of irradiation eliminates the possible questions about heating induced by rf power.

III. EFFECT OF LOW-FREQUENCY AC VOLTAGE ON THE SHAPE OF *I-V* CURVES

Below 50 MHz, the ac voltage across the sample is not significantly different from the output voltage of the generator. This can be directly controlled by an oscilloscope. Therefore, we have compared the effect of ac voltage at different frequencies for a given amplitude.

The measurements were performed on a NbS_3 nanosample at room temperature in the frequency range of 0.2–50 MHz. The amplitude of the voltage was 170 mV, somewhat above V_t.

Figure 1 shows the $\sigma_d(V)$ curves obtained. At $f < 5$ MHz, the "trivial" frequency independent effect can be seen: this is just smearing out of the I-V curve due to averaging over the range $\pm\delta V$, where δV is the amplitude of the ac signal. However, already for 10-MHz irradiation, the curve begins to acquire a threshold shape. Note that this is not just approaching the nonperturbed $\sigma_d(V)$ curve. One can see that for 50-MHz irradiation, σ_d above the threshold increases faster than without

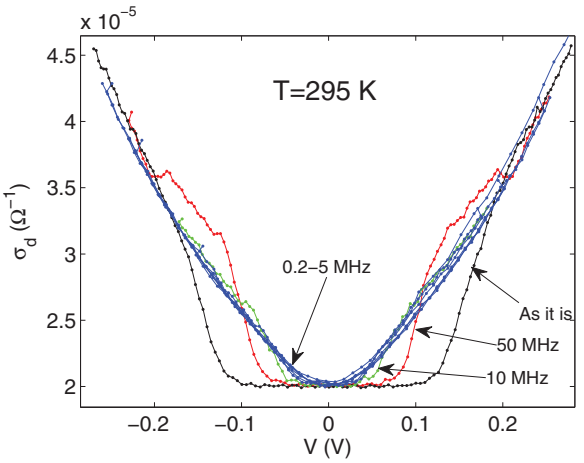

FIG. 1. (Color online) The $\sigma_d(V)$ curves of the NbS_3 sample (28×0.26 μm^2) without ac voltage and under irradiation at $f = 0.2$, 0.5, 1, 2, 5, 10, and 50 MHz. The span of the ac voltage is $\pm$170 mV (the Shapiro steps can be seen on the 50-MHz curve).

irradiation. Below, we demonstrate that this tendency in the evolution of the $\sigma_d(V)$ dependencies is still more visible for higher frequencies.

IV. EFFECTS OF RF IRRADIATION ON THE SHAPE OF THE *I-V* CURVES OF NbS_3

Figure 2(a) presents examples of $\sigma_d(V)$ curves for the NbS_3 nanosample as it is and under irradiation at two frequencies (in both cases the value of V_t is suppressed down to zero). One can see Shapiro steps whose positions in the current correspond with the values of f.[5] However, we are drawing attention to the shape of the curves near V_t. Note that without irradiation, σ_d grows gradually. The higher f is, the sharper the depinning of the CDW: one can see an increase in both $d\sigma_d/dV$ and the amplitude of the steep growth of σ_d. Under the 600-MHz irradiation, σ_d rapidly increases at $V > V_t$, nearly four times, and approaches the value of ohmic conductivity above the 360-K Peierls transition. Similar consequences of rf irradiation are clearly seen from Fig. 2(b). The sharpening of the CDW depinning under rf irradiation can be found in some earlier papers (see Fig. 2 in Ref. 12, as an example), but this effect has not been discussed.

In some (perfect) samples, the CDW depinning is sharp even without cohering irradiation (even negative differential resistance of the CDW can be seen above the threshold[13]). In this case the effect of irradiation is not so pronounced, but the amplitude of the steep growth of σ_d is strongly increased as well.

V. THE SHAPIRO STEPS UNDER COHERING RF IRRADIATION OF NbS_3

To probe the state of the CDW sliding above E_t, one can either study the noise or rf interference. In this paper, we concentrated on the rf studies. Figure 3(a) shows curves similar to those in Fig. 2 for a sample under relatively low-frequency irradiation (25 MHz) of different amplitudes. Clearly, the sharpness of the CDW depinning grows rather faintly, even if the rf voltage is far above the threshold. Figure 3(b) shows

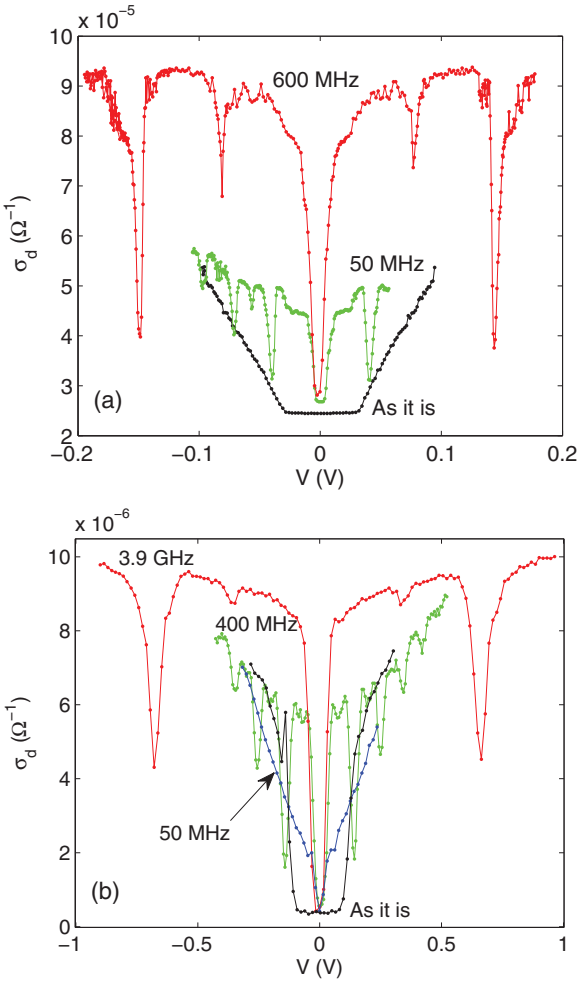

FIG. 2. (Color online) (a) Differential conductivity of the NbS_3 sample vs V without irradiation and under 50- and 600-MHz irradiation (sample 1, $7.5 \times 0.08\ \mu m^2$). (b) Similar curves for another sample under irradiation of 50-, 400-, and 3874-MHz (sample 2, $6.5 \times 0.0077\ \mu m^2$).

σ_d vs V curves with cohering 400-MHz irradiation and without it; in both cases synchronizing 25-MHz irradiation is applied for testing the CDW coherence. Although without 400-MHz "pumping", the Shapiro steps are faintly defined, they become quite pronounced with the help of the 400-MHz power. Note that the positions of the Shapiro peaks are the same if we plot σ_d as a function of nonlinear current [Fig. 3(c)].

Thus, we can conclude that the rf power stimulates coherence not only on the CDW depinning but also on the CDW sliding.

VI. THE EFFECTS OF COHERING RF IRRADIATION ON $(TaSe_4)_2I$ AND TaS_3

The stimulation of the CDW coherence can be observed not only for NbS_3. Figure 4 shows the effect of rf on a thin sample of $(TaSe_4)_2I$. With the increase of the rf frequency, the tendency is similar to that found for NbS_3: the gain of the CDW velocity becomes more abrupt in voltage.

The CDW in $(TaSe_4)_2I$ is known to show poor coherence. The peaks of NBN are rather wide ($\delta f_f / f_f \geqslant 1/10$),[14,15] and no synchronization under rf has been previously reported.

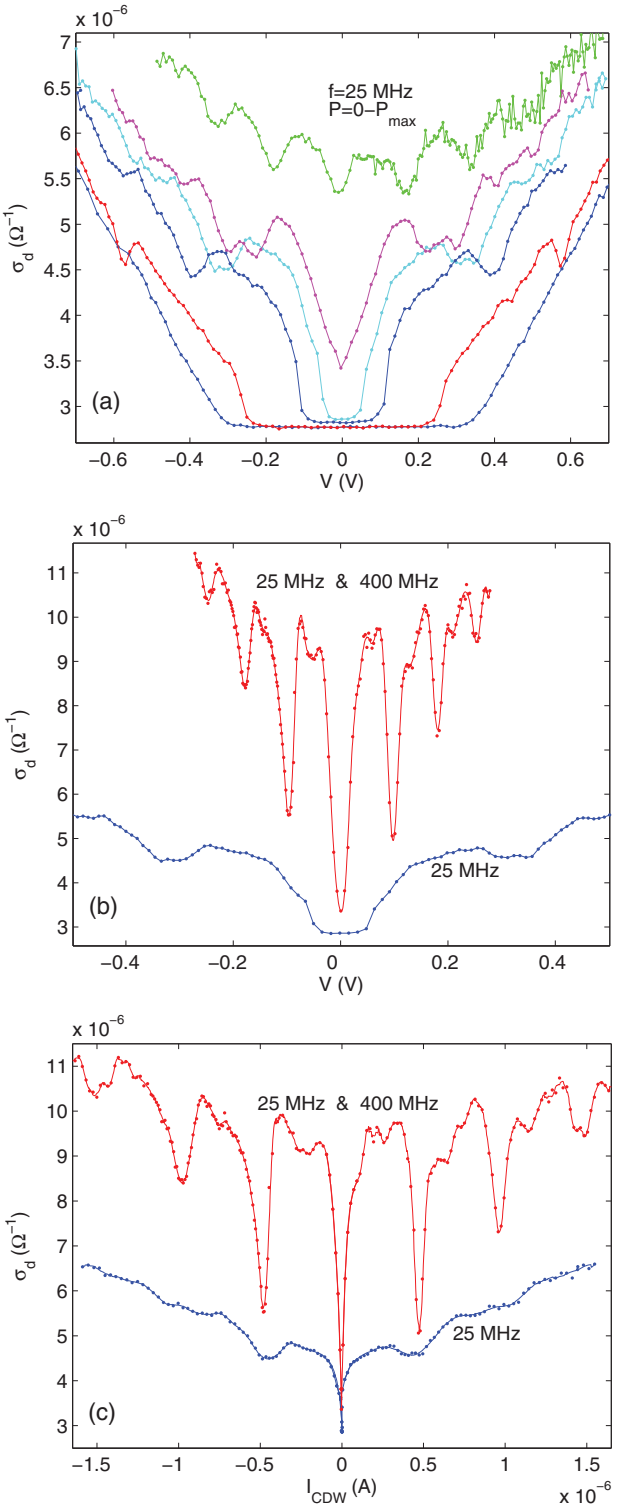

FIG. 3. (Color online) $\sigma_d(V)$ curves for a NbS_3 nanosample under 25-MHz irradiation. (a) Under different power without cohering irradiation. (b) For the upper curve, 400-MHz radiation is applied in addition. (c) The data from (b) as a function of nonlinear current. The sample dimensions are $55 \times 0.1\ \mu m^2$.

Selecting of thin samples or cleaving of large crystals allowed us to increase the CDW coherence (see Fig. 4 for example). Figure 5 shows $\sigma_d(V)$ curves for the same sample under 20-MHz "synchronizing" irradiation. For one of the curves,

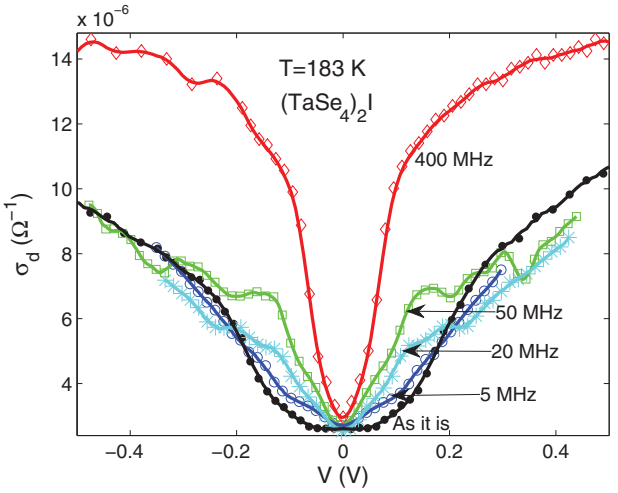

FIG. 4. (Color online) Effect of rf irradiation at different frequencies (indicated in the plot) on the $\sigma_d(V)$ dependence for a $(TaSe_4)_2I$ sample ($24 \times 0.05\ \mu m^2$).

cohering 400-MHz irradiation is applied. One can see hints of the Shapiro peaks (shown with arrows) even without extra radiation; the 400-MHz irradiation makes the peaks obvious.

Similar results are obtained for the widely studied compound TaS_3.[1] Figure 6 shows the effect of cohering irradiation with $f = 400$ MHz. Without it, no hints of synchronization can be seen under 2-MHz ac voltage, whereas the cohering radiation makes the peaks obvious. Thus, in some cases, additional superhigh frequency irradiation allows observation of Shapiro steps, which are invisible otherwise.

VII. THE EFFECTS OF COHERING IRRADIATION ON THE NBN AND BBN

The synchronizing radiation always distorts the CDW dynamics, while the noise characterizes it as it is. Therefore,

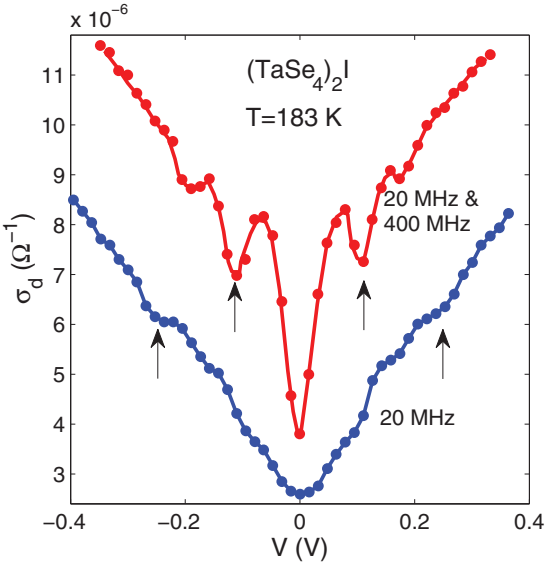

FIG. 5. (Color online) $\sigma_d(V)$ curves for $(TaSe_4)_2I$ under 20-MHz irradiation. For the upper curve (cohering), 400-MHz radiation is applied in addition. The arrows help to see the Shapiro steps. The solid lines are guides for the eyes. $T = 183$ K.

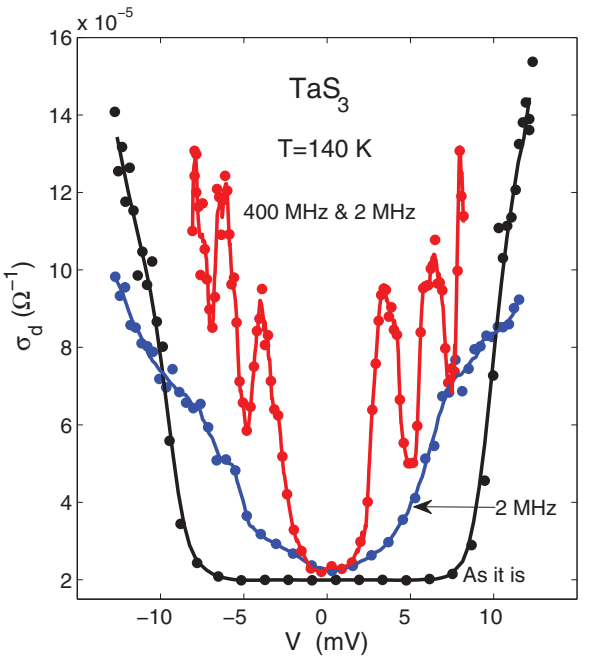

FIG. 6. (Color online) $\sigma_d(V)$ curves for a TaS_3 sample as it is and under 2-MHz synchronizing irradiation (with and without 400-MHz cohering irradiation). The solid lines are guides for the eyes. The sample dimensions are $28 \times 0.11\ \mu m^2$.

the character of NBN and BBN is the most direct indicator of the degree of coherence of sliding CDW.

For studies of NBN, we selected TaS_3, the compound in which the experiment is simplest in arrangement. We have noticed that the typical frequencies, either cohering or synchronizing, are lower for $(TaSe_4)_2I$ and, especially, for TaS_3 than for NbS_3. Generally speaking, NbS_3 can be considered a "high-frequency" compound: the highest frequencies of CDW synchronization approach 20 GHz[5–7] and are limited by the matching of rf power with the samples. Some considerations about the reason for this are presented in Refs. 6 and 7, though the answer is still far from clear.

Alternatively, TaS_3 can be called a "low-frequency" compound. This concerns NBN as well: among the compounds considered in this paper, TaS_3 shows the lowest frequencies of NBN. The corresponding peaks in the noise spectra can be observed without involving a high-impedance high-frequency amplifier.

Figure 7 shows examples of power spectra obtained by means of fast Fourier transform of noise time domains for a TaS_3 sample. The spectra (a) and (b) are recorded at two different values of the CDW current, corresponding with $f_f = 0.16$ and 0.37 MHz, respectively. Each panel presents spectra under cohering 400-MHz irradiation and without it. The lower curves (shifted down by 30 dB) are obtained under the 400-MHz radiation. From Fig. 7, one can see that the cohering radiation strongly affects the NBN. The peaks in both panels become sharper and higher under the irradiation. The irradiation removes splitting of the NBN lines. Moreover, new lines can be seen: in the upper panel, the third harmonic and in the lower panel, the second harmonic, together with first subharmonic, become visible. This result directly shows that

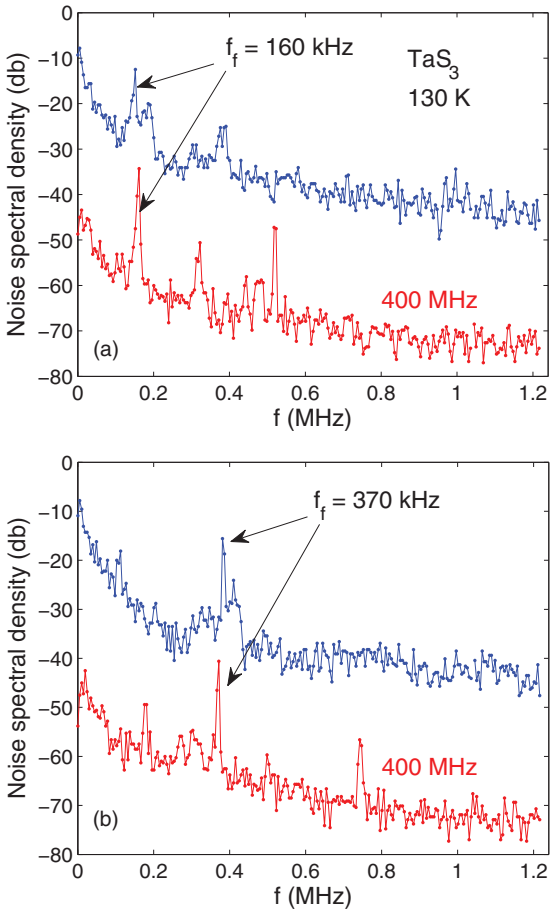

FIG. 7. (Color online) Power spectra of noise for a TaS_3 sample. The lower curves in each panel are obtained under 400-MHz irradiation, and the upper ones without it. The current is tuned so that $f_f = 0.16$ MHz for both curves in the upper panel, and 0.37 MHz in the lower one. The lower curves are shifted by 30 dB downward). At frequencies below ~10 kHz, the noise is suppressed by a cutoff filter. The sample dimensions are $60 \times 0.58\ \mu m^2$.

the CDW sliding becomes more coherent under asynchronous rf irradiation.

In Fig. 7, one can also notice that the irradiation suppresses the level of BBN at the lowest frequencies. This is better seen from Fig. 8, where similar spectra are presented at lower currents and without vertical shift. Suppression of BBN is observed also for NbS_3 samples.

We should note that the cohering irradiation decreases the whole level of noise, but, of course, the noise suppression is stronger within the synchronized modes. This can be seen from Fig. 9, where low-frequency noise voltage is plotted as a function of current (a), as well as $\sigma_d(I)$ curves (b) for a NbS_3 sample. On average, the noise level is notably lower for the irradiated sample, but additional dips of noise voltage are seen at the currents corresponding to the Shapiro steps. This could be expected, because synchronization denotes that the CDW is sliding uniformly, as a whole. The drop of the BBN noise level is also in concordance with the narrowing of NBN in the synchronized mode reported in Ref. 16.

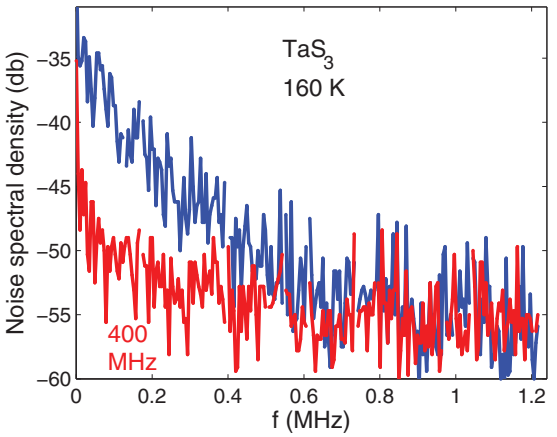

FIG. 8. (Color online) Power spectra of noise for a TaS_3 sample at current slightly above I_t. The upper curve is without irradiation and the lower one is under 400-MHz irradiation. The sample dimensions are $16 \times 0.066\ \mu m^2$.

VIII. DISCUSSION

The experiments presented above show that under rf irradiation, the depinning of the CDW at the threshold field becomes more synchronous, and its sliding becomes more

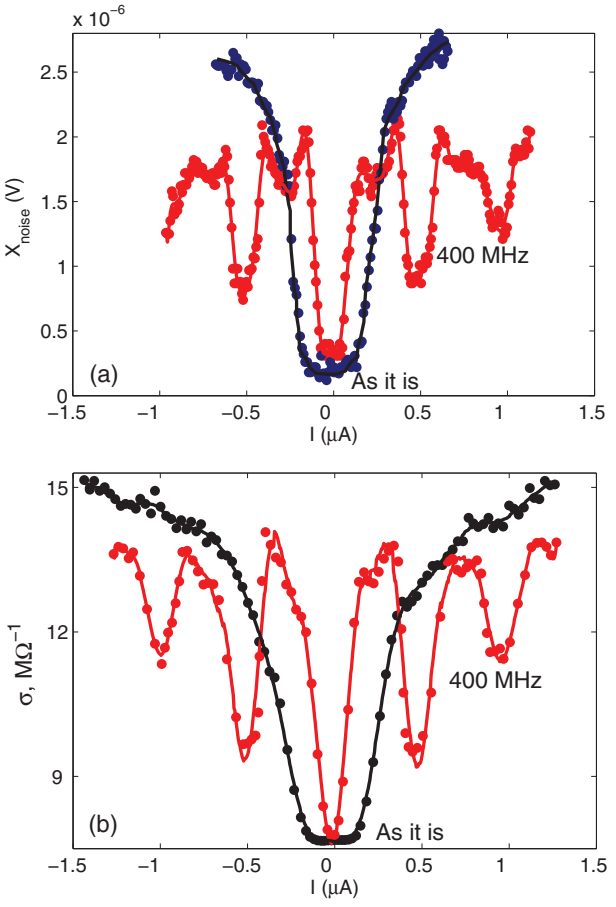

FIG. 9. (Color online) (a) Noise voltage at 33 Hz for the NbS_3 sample as a function of current: unradiated and under 400-MHz irradiation. (b) The $\sigma_d(I)$ curves in the same conditions. The sample dimensions are $5 \times 0.0046\ \mu m^2$.

coherent. The high value of the CDW differential conductivity indicates that the rf power strongly suppresses the damping of the CDW.

To understand the effects of rf irradiation observed, it is worth recalling another feature of the CDW dynamics, the high amplitude of the transient voltage oscillations just after application of a current pulse $I > I_t$, known also as transient "ringing".[10,11,17] The time domains of voltage show oscillations at the fundamental frequency on top of the pulse. The central issue reported is that several first oscillations are of extremely large amplitude, which is a percentage of the dc voltage applied. The amplitude of the following oscillations decreases, and finally they become (nearly) indistinguishable. Though this effect has no quantitative explanation, its origin is quite clear. Different CDW domains start sliding from the same initial phase with respect to the pinning potential, corresponding to the minima of their energies. Therefore, at first the phases of the domains show similar time dependencies. However, because the domains slide at slightly different velocities, the phase synchronism vanishes. This resembles the picture of competitions in hurdling: at first, just after the start, the sportsmen jump the barriers synchronously, but later, they fall out of sync.

The high initial amplitude of NBN demonstrates the principle possibility of highly coherent CDW sliding. The CDW would go on sliding without loss of coherence if some external impact would enforce all the domains to return to the initial configuration after surmounting each barrier. It is natural to suppose that the rf irradiation is such an impact. The superhigh frequency field allows relaxation of metastable states at time scales much shorter than the inverse washboard frequency. Thus, the rf field helps to restore the CDW equilibrium configuration after each advancement by λ. We should note that relaxation of metastable states of the CDW and the acceleration of the process under electric field were previously studied both experimentally[18–20] and theoretically;[21,22] in Ref. 22, the picture of local metastable states was applied to kinetics of the CDW. Also, the rf electric field with decreasing amplitude was used to erase remnant CDW deformations due to sample history in the synchrotron x-ray studies of $NbSe_3$.[23]

The close mechanical analogy is transformation of solid friction into the viscous flow induced by mechanical vibrations.[24] This "viscous" friction of the CDW allows the domains to slip back into the potential wells (configuration close to equilibrium) after surmounting each barrier. In other words, the cohering irradiation prevents the CDW from breaking into domains sliding independently.

Similar consideration concerns depinning. It is known that single-domain samples show negative differential resistance on depinning.[13] Correspondingly, smearing out of the $\sigma_d(V)$ curves at V_t reveals incoherent depinning of different domains. The cohering irradiation reduces the "solid" friction and enables onset of the CDW sliding as a whole.

What should be the frequency of the cohering irradiation? Clearly, for the given current, the irradiation frequency should be of the order or above the fundamental frequency. The higher the frequency is, the higher is the number of "attempts" of the CDW to approach the equilibrium before it advances to the next wavelength.

With this explanation, it is also possible to understand, why the high-frequency irradiation does not smear out the $\sigma_d(V)$ curves at low voltages, i.e., near the threshold. As long as f_f is below the rf frequency f, the time of the rf impact, $\sim 1/f$, is too short for the CDW (because of its inertia) to advance by extra wavelength or, vice versa, to fall behind by λ. This can explain the recovery of the threshold character of the curves with f increase, seen in Fig. 1. At the same time, as far as the ac voltage is comparable with E_t or even exceeds it, the instantaneous values of voltage can strongly exceed the dc value, therefore high-voltage sliding states ($f_f > f$) contribute to the conductivity. In this case, the time $\sim 1/f$ of the high voltage impact is enough to advance the CDW by one or more periods. That is why the conductivity under ac interference can be much higher than without it.

These qualitative considerations can give the idea of the treatment of the I-V curves under microwave irradiation. We should also add that empirically, strong cohering effect is produced by irradiation, which induces pronounced Shapiro steps (in case the appropriate current is achieved).

In conclusion, we have found that under rf irradiation, both depinning and sliding of the CDW in different compounds become more coherent. This can be seen from the shape of the I-V curves, from synchronization by another rf source, from narrowing of NBN lines, and from suppression of BBN. With voltage growth, the irradiated CDW gains the velocity above the threshold much faster and slides with much lower dissipation. The higher the frequency is, the more pronounced the effect is. The coherence of the CDW can be explained by the effect of rf irradiation on the relaxation of metastable states forming at the CDW sliding.

The effect has immediate application: it allows studies of coherent CDW sliding and Shapiro steps at record low velocity and/or rf voltage and in the samples/compounds, where otherwise they are unobservable (see Fig. 5 as an example). This increase of the sensitivity of the I-V curves to the synchronizing irradiation can be important if one employs the CDW conductors as rf receivers with spectral resolution. Sharpening of the I-V curves at E_t also helped us to prove that the second threshold for nonlinear conductivity in NbS_3 at 300 K is associated with depinning of the ultrahigh temperature CDW, with T_{P0} above 600 K.[25]

ACKNOWLEDGMENTS

We are grateful to R. E. Thorne and F. Levy for granting the high-quality samples and to S. V. Zaitsev-Zotov and V. F. Nasretdinova for helpful discussions. The support of the Russian Foundation for Basic Research, "New materials and structures" of the Russian Academy of Sciences programs, and the Ministry of Science and Education of Russia (Agreement No. 8571) is acknowledged. This work was performed in the framework of the Associated European Laboratory "Physical properties of coherent electronic states in condensed matter," including Département Matière Condensée-Basses Températures and Kotel'nikov Institute of Radioengineering and Electronics.

*pok@cplire.ru

[1]P. Monceau, Adv. Phys. **61**, 325 (2012).
[2]N. P. Ong and K. Maki, Phys. Rev. B **32**, 6582 (1985).
[3]L. P. Gor'kov, Pis'ma Zh. Eksp. Teor. Fiz. **38**, 76 (1983) [Zh. Eksp. Teor. Fiz. **86**, 1818 (1984)].
[4]S. Brown and A. Zettl, in *Charge Density Waves in Solids*, edited by L. P. Gor'kov and G. Grüner (Elsevier, Amsterdam: North-Holland, 1989), Vol. 25, p. 223.
[5]S. G. Zybtsev, V. Ya. Pokrovskii, V. F. Nasretdinova, and S. V. Zaitsev-Zotov, Appl. Phys. Lett. **94**, 152112 (2009).
[6]S. G. Zybtsev, V. Ya. Pokrovskii, S. V. Zaitsev-Zotov, and V. F. Nasretdinova, Physica B **407**, 1696 (2012).
[7]V. Ya. Pokrovskii, S. G. Zybtsev, M. V. Nikitin, I. G. Gorlova, V. F. Nasretdinova, and S. V. Zaitsev-Zotov, Usp. Fiz. Nauk **183**, 33 (2013) [Phys. Usp. **56**, 29 (2013)].
[8]J. McCarten, D. A. DiCarlo, M. P. Maher, T. L. Adelman, and R. E. Thorne, Phys Rev B **46**, 4456 (1992).
[9]S. V. Zaitsev-Zotov, Usp. Fiz. Nauk **174**, 585 (2004) [Phys. Usp. **47**, 533 (2004)].
[10]R. M. Fleming, L. F. Schneemeyer, and R. J. Cava, Phys. Rev. B **31**, 1181 (1985).
[11]P. Parilla and A. Zettl, Phys. Rev. B **32**, 8427 (1985).
[12]L. C. Bourne, M. S. Sherwin, and A. Zettl, Phys. Rev. Lett. **56**, 1952 (1986).
[13]D. V. Borodin, S. V. Zaitsev-Zotov, and F. Ya. Nad', Zh. Eksp. Teor. Fiz. **90**, 318 (1986) [JETP **63**, 184 (1986)].
[14]Z. Z. Wang, M. C. Saint Lager, P. Monceau, M. Renard, P. Gressier, A. Meerschaut, L. Guemas, and J. Rouxel, Solid State Commun. **46**, 325 (1983).
[15]G. Mozurkewich, K. Maki, and G. Grüner, Solid State Commun. **48**, 453 (1983).
[16]R. E. Thorne, J. S. Hubacek, W. G. Lyons, J. W. Lyding, and J. R. Tucker, Phys. Rev. B **37**, 10055 (1988).
[17]B. Fisher, Phys. Rev. B **30**, 1073 (1984).
[18]D. M. Duggan, T. W. Jing, N. P. Ong, and P. A. Lee, Phys. Rev. B **32**, 1397 (1985).
[19]G. Mihály, A. Jánossy, and G. Kriza, Lect. Notes Phys. **217**, 396 (1985).
[20]S. V. Zaitsev-Zotov, Synth. Met. **43**, 3923 (1991).
[21]A. B. Kolton, A. Rosso, T. Giamarchi, and W. Krauth, Phys. Rev. Lett. **97**, 057001 (2006).
[22]S. Brazovskii and T. Nattermann, Adv. Phys. **53**, 177 (2004); **53**, 1011(E) (2004).
[23]H. Requardt, F. Ya. Nad, P. Monceau, R. Currat, J. E. Lorenzo, S. Brazovskii, N. Kirova, G. Grübel, and Ch. Vettier, Phys. Rev. Lett. **80**, 5631 (1998).
[24]Ilija. I. Blekhman, *Vibrational Mechanics: Nonlinear Dynamic Effects, General Approaches, Applications* (World Scientific Publishing Co. Pte. Ltd., Singapore, 2000).
[25]S. G. Zybtsev, V. Ya. Pokrovskii, S. V. Zaitsev-Zotov, and V. F. Nasretdinova (unpublished).